PHYSICAL REVIEW A VOLUME 19, NUMBER 1 JANUARY 1979

Electroclinic effect at the A-C phase change in a chiral smectic liquid crystal

Stephen Garoff* and Robert B. Meyer
Division of Applied Science, Harvard University, Cambridge, Massachusetts 02138
(Received 30 June 1978)

When a smectic-A phase is composed of chiral molecules, it exhibits an electroclinic effect, i.e., a direct coupling of molecular tilt to applied field. The pretransitional behavior of the electroclinic effect in the A phase is used to study the critical behavior near the second-order, smectic-A–smectic-C phase transition. This behavior is measured by monitoring the change in birefringence of a sample as the electroclinic effect causes a tilt of the molecules. A large pretransitional effect is measured, and constants describing the critical behavior are determined.

INTRODUCTION

Meyer *et al.*[1] established the existence and behavior of ferroelectric liquid crystals. Since then many of the properties of these liquid crystals have been investigated: synthesis and properties of several compounds which have enhanced ferroelectric properties,[2] polarization, tilt angle, and helical pitch[3-5]; shear-induced polarization[6,7]; pyroelectricity[8]; properties of thin films[9,10]; and theoretical discussions of the ferroelectric phase[11] and the phase transition.[12,13] As previously reported,[14] our experiment is a measurement of a new phenomenon—the electroclinic (EC) effect. This effect occurs when an electric field applied parallel to the smectic layers induces a molecular tilt relative to the layer normal. Using the EC response, we probe the critical behavior on the smectic-A side of the chiral smectic-A–smectic-C phase transition. This work is one of the first detailed studies of the critical properties of this phase transition. Our results raise some question about the exact nature of the phase change. In this paper we will describe the theoretical and experimental details of our work.

I. ORIGIN OF EC EFFECT

A symmetry argument, similar to that predicting ferroelectricity in a chiral smectic C,[1] describes the origin of the EC effect in a smectic-A phase composed of chiral molecules. The chiral smectic-A phase is uniaxial with the long molecular axis or director $\hat{d}$ parallel to the normal to the smectic layers $\hat{n}$ and a twofold axis perpendicular to the molecules. The molecules are free to rotate about their long axis. If an electric field E is applied parallel to the smectic layers, this free rotation is biased due to the tendency of the transverse component of the permanent molecular dipole P to orient parallel to the field. The system maintains a twofold axis along the electric field. In a nonchiral system, the plane containing $\hat{n}$ and P is a mirror plane. However, the chirality of the phase destroys all mirror symmetries. Therefore, the free energy for molecular tilt is no longer symmetric about the $\hat{n}P$ plane and a molecular tilt is induced in a plane perpendicular to the $\hat{n}P$ plane. This linear connection between the polarization and induced tilt represents the EC response of the chiral smectic-A phase.

Although the EC effect in the chiral smectic phase is very closely related to the piezoelectric effect in crystalline phases, we use a distinctive name because the fluid nature of the liquid crystalline phase cannot support the static shear stains associated with piezoelectricity. Mechanistically, the atomic reorientations developed in the unit cell of the piezoelectric crystal displace neighboring unit cells; however, the molecules in one smectic layer tilt under the influence of the EC effect without affecting the adjacent layers

II. CRITICAL BEHAVIOR OF EC RESPONSE

The chiral smectic-A–smectic-C phase change is second order.[1] Both x-ray and optical measurements have shown that the tilt angle θ goes to zero at the critical temperature T_c.[3] The helical pitch of the chiral smectic-C phase has not been measured near T_c. While existing measurements indicate that the pitch is rapidly decreasing as T_c is approached,[15] the pitch may be zero at T_c or it may be some small but finite value. As will be discussed below, the transition is characterized by an incomplete divergence of the EC coefficient and the electric polarization susceptibility.

The critical behavior at the chiral smectic-A–smectic-C transition is predominated by the intermolecular forces inducing the nonchiral smectic-C phase. The energies involved in the spontaneous polarization and the helical structure of the chiral case are minor perturbations on these nonchiral energies. The fact that the polarization and helix are small perturbations is evidenced by

the fact the nonchiral transition temperature in the racemic mixture of p-decyloxybenzylidene-p'-amino-2-methylbutylcinnamate (DOBAMBC) is only about 1 °C below the chiral transition temperature T_c of the pure chiral compound. Therefore, the true divergent susceptibility of the transition (i.e., the susceptibility connected with the order parameter) is dominated by the behavior of A, the susceptibility controlling the tilt of the director. As will be seen in the following paragraphs, this susceptibility controlling the tilt is renormalized by the presence of the spontaneous polarization. Further, the effects of the helix on the various susceptibilities in the chiral smectic-A phase may be ignored except in a very small temperature regime ΔT near T_c. In this regime of the chiral smectic-A phase, the correlation length of the fluctuations is comparable to the pitch of the helical structure in the fluctuations.

The behavior of the EC response can best be examined by considering the static spacially homogeneous free-energy density of the chiral smectic-A phase. As mentioned above, such a spacially homogeneous free energy may be used throughout the smectic-A phase except in the small region ΔT near T_c where effects of the helical structure of the fluctuations significantly alter the free energy. If the electric field is applied parallel to the smectic layers and no shear stress is present, then the free energy density can be written

$$g = g_0 + \tfrac{1}{2}A'(T)\theta^2 + \cdots + \tfrac{1}{2}\chi_P^{-1}P^2 - (1/8\Pi)\epsilon^0 E - PE + t\theta P\,, \qquad (1)$$

where g_0 represents contributions to g from the undisturbed smectic A. θ is the molecular tilt normal to E; P is the component of the average molecular polarization parallel to E; ϵ^0 is the dielectric constant without contributions from the permanent dipole, χ_P is a generalized susceptibility, and t is the electroclinic coupling constant. A' goes to zero at T_0 the transition temperature for the racemic mixture. The term $\chi_P^{-1}P^2$ is the lowest-order term in P (by summetry considerations). The magnitude of this term is due to entropic effects and steric and dipole-dipole interactions.[16] (The need for this term is best exhibited when considering the increase in free energy by a shear-induced polarization with no applied field.) The electroclinic coupling is seen in the final term of Eq. (1). This form of free energy is common to a class of materials called pseudo-proper ferroelectrics such as $(NH_4)_2SO_4$.[17,18]

Since P and θ are independent variables, their equilibrium values are found by setting $\partial g/\partial P$ and $\partial g/\partial\theta$ separately equal to 0. This gives the following results:

$$g = g_0 + \tfrac{1}{2}A\theta^2 - (1/8\pi)(\epsilon^0 + 4\pi\chi_P)E^2 - t\chi_P E\theta \qquad (2)$$

where

$$A = A' - \tfrac{1}{2}\chi_P t^2 \qquad (3)$$

and

$$\theta = t\chi_P E/A \qquad (4)$$

$$\epsilon = \epsilon^0 + 4\pi\chi_P + 4\pi(\chi_P t)^2/A\,. \qquad (5)$$

The new susceptibility A goes toward zero at a temperature T' which is ΔT below T_c, the chiral transition temperature. However, this softening of the susceptibility is incomplete and is truncated in the temperature regime ΔT discussed above. The modification of this susceptibility indicated in Eq. (3) leads to a renormalization of the transition temperature from T_0 for the nonchiral transition. This renormalization is just due to the coupling of P to θ. θ is linear in the applied field and the EC response diverges as A^{-1}. The dielectric constant ϵ contains a contribution which diverges toward T'. Despite the truncation of the divergence of ϵ within ΔT of T_c, the behavior is reminiscent of a Curie point in crystalline ferroelectrics.

Therefore, three temperatures T_0 (the nonchiral transition temperaure), T_c (the chiral transition), and T' (the temperature toward which the susceptibility A diverges) are imporatnt. As mentioned, the renormalization from T_0 to T_c is primarily due to the coupling of P to θ. The truncations of the divergence of the EC response and ϵ are due to a helical structure appearing within the fluctuations. When a helical structure exists in a fluctuation, a small electric field cannot produce a net dipole moment in the fluctuation. In contrast, away from the transition in the smectic-A phase, a small electric field can bias the rotation of the molecules about their long axis and can produce a net polarization. Thus the response of the system to the electric field must change when passing from the regime where a small electric field produces a net polarization throughout the sample to the regime—within ΔT of T_c—where a small field cannot produce a net polarization within fluctuations which now exhibit a helical structure. This alteration of the response is described by the truncation of the divergence of the EC response and of ϵ within ΔT of T_c. Outside ΔT, the simple free energy described by Eqs. (1)–(5) adequately describes the system.

On the smectic-A side of the chiral transition, A goes toward 0 as some power law

$$A = a[(T - T')/T']^{\gamma}\,. \qquad (6)$$

Except within ΔT $(= T_c - T')$ of the actual transition, A accurately approximates the true diver-

gent susceptibility of the chiral smectic-A–smectic-C transition. Therefore, insight may be gained by the comprison of the γ in Eq. (6) with the exponent governing the divergence of the susceptibility conjugate to the order parameter in other transitions of the same universality class.

Because of the overall symmetry properties of the nonchiral smectic-A–smectic-C phase change, de Gennes has drawn an analogy between this transition and the normal-to-superfluid transition in ^{4}He.[19] An XY ferromagnet (a ferromagnet with three spin components but one completely uncoupled) is another system with the same symmetry. In the high-temperature-series analysis, the asymptotic values for γ are 1.0 in the mean-field limit (far from the transition) and 1.315 near the transition.[20] This type of analysis has been extended to calculate the crossover between these asymptotic limits.[21] A possible breakdown of the analogy may occur due to the polar—and perhaps chiral—symmetry of the low-temperature phase in the chiral smectic-A–smectic-C transition.

III. DYNAMIC BEHAVIOR OF THE EC RESPONSE

Although the divergence of A is most clearly seen for a dc applied field, electrohydrodynamic effects prohibit the dc experiment. Therefore, the dynamic response of the system must be examined. A phenomenological equation of motion for θ under the influence of an electric field is

$$\Gamma\dot{\theta}+A\theta=cE\,, \tag{7}$$

where Γ is a viscosity and $c=\chi_P t$ is the coupling constant between θ and E. Although there have been some predictions of very weak critical behavior in Γ near the smectic-A–smectic-C transition (with an exponent on the order of 0.05),[22] Γ will be assumed to show only a simple Arrhenius form

$$\Gamma=\Gamma_0 e^{B/T}\,, \tag{8}$$

where B is an activation energy in units of Boltzmann's constant. Frequency and temperature dependences in c will be neglected.

If E is sinusoidal with angular frequency ω, then the induced tilt is described by an amplitude θ_0 and a phase δ

$$\theta_0=cE/(A^2+\omega^2\Gamma^2)^{1/2}\,, \tag{9}$$

$$\delta=\tan^{-1}(-\omega\Gamma/A)\,. \tag{10}$$

Because of the critical behavior of A, the electroclinic response should show the following features: (i) as T approaches T', the amplitude rises and the phase shifts through $-90°$; (ii) near T', the viscosity term in the amplitude dominates and the response is strongly frequency dependent; (iii) far from T', the elastic term is dominant and the response shows dispersion only at high frequencies.

The relaxation time for a thermal fluctuation of the tilt angle is

$$\tau=\Gamma/A\,. \tag{11}$$

Since τ diverges as $(T-T')^{-\gamma}$ in the smectic-A phase as the transition is approached, critical slowing of the fluctuations occurs. This divergence has been seen in a light scattering experiment at the nonchiral smectic-A–smectic-C transition.[23]

IV. ELECTRO-OPTICAL RESPONSE

In an aligned smectic-A sample, the optic axis is along the long molecular axis. Therefore, an applied electric field induces a tilt of the optic axis through the molecular tilt of the EC response. (For small tilts, the sample remains essentially uniaxial.) This tilt of the optic axis produces a modulation of the birefringence of the sample. Monitoring the amplitude and phase (relative to the applied field) of this electro-optical effect is a direct measure of the amplitude and phase of the EC response and therefore is a probe of the critical phenomena at the smectic-A–smectic-C transition.

This modulation is best measured by placing the sample between crossed polarizers and measuring the transmission of the system with a laser beam passing through the sample at an oblique angle. The sensitivity of this method is maximized by choosing the largest practical angle of incidence such that the output beam from the sample is circularly polarized (i.e., at the half-maximum intensity point of a ring on the uniaxial conoscopic image) and by selecting the input polarization to produce equal amplitudes in the ordinary and extraordinary rays in the sample (i.e., at 45° to the arms of the uniaxial cross of the conoscopic image). Using this operating point and phase-sensitive detection, coherent molecular tilts as small as 5 μ rad are easily measured. With this sensitivity, the EC effect can be measured 10–15 K above T_c with only small applied fields.

V. EXPERIMENTAL SET UP AND PROCEDURES

The chiral compound used was p-decyloxbenzylidene-p'-amino-2-methylbutylcinnamate (DOBAMBC). The phase diagram for this compound is

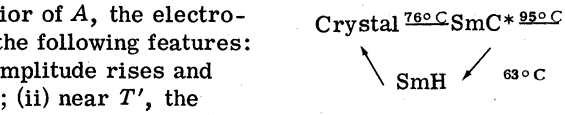

Since the smectic-A phase has a large temperature range, effects from the isotropic phase should not

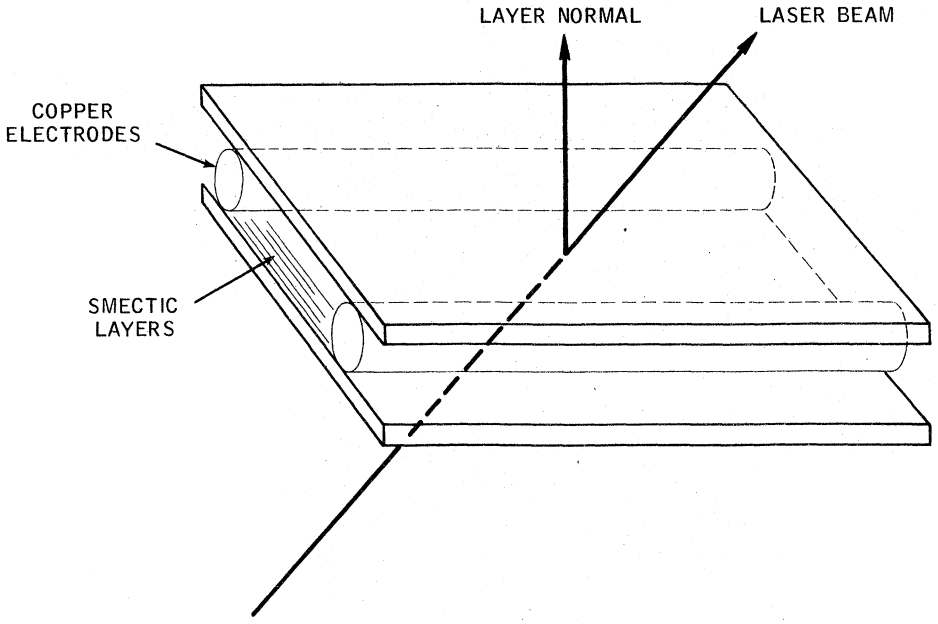

FIG. 1. Sample geometry.

influence the critical behavior at the chiral smectic-*A*–smectic-*C* transition. The absence of a cholesteric phase above the smectic-*A* phase facilitates the production of aligned samples.

In the sample geometry shown in Fig. 1, the copper wires, which are 116 μm in diameter and 1.5 mm apart, act both as electrodes and spacers. The homeotropic alignment is produced by use of hexadecyltrimethyl ammonium bromide surfactant. For this geometry, the EC effect causes a molecular tilt in the plane of incidence of the light.

The block diagram of the optical apparatus is shown in Fig. 2. The sample is mounted in the sample oven such that the wires of the sample are parallel to the plane of incidence. Set at 45° to the plane of incidence, polarizer A minimizes intensity variations due to mode hopping of the laser. Since the reflection coefficient of the beam splitter is polarization dependent, polarizer A also insures that the reflectivity of the splitter is constant despite any polarization changes in the laser. The laser monitor allows normalization of the electro-optic signal against variations in the laser output. Polarizer B—set parallel to polarizer A—and polarizer C are crossed and allow measurement of the modulated birefringence of the sample. In order to monitor the condition of the sample during the experiment, a long working distance microscope and a light source are used.

Flushed with dry nitrogen, the two-stage sample oven provides a controlled environment for the sample. The temperature control provided by the

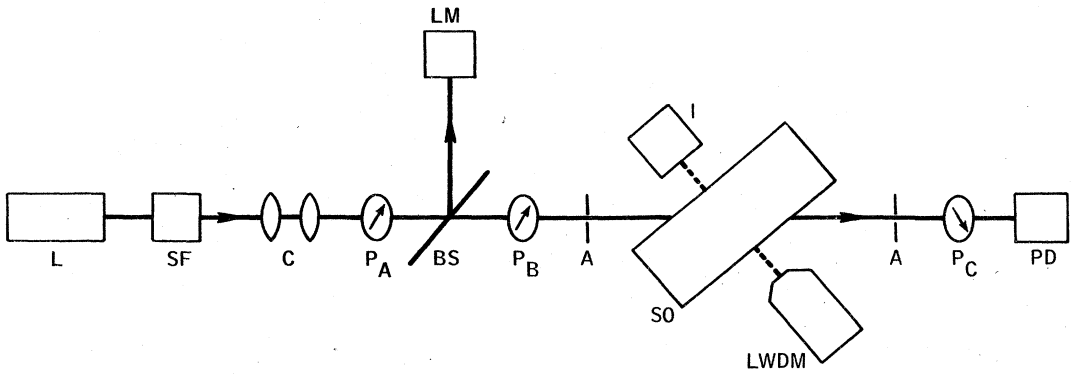

FIG. 2. Block diagram of optical apparatus: A, apertures; BS, beam splitter; C, columator; I, illuminator; L, laser; LM, laser monitor; LWDM, long working distance microscope; P_A, P_B, P_C, polarizers; PD, photodiode; SF spatial filter; SO, sample oven.

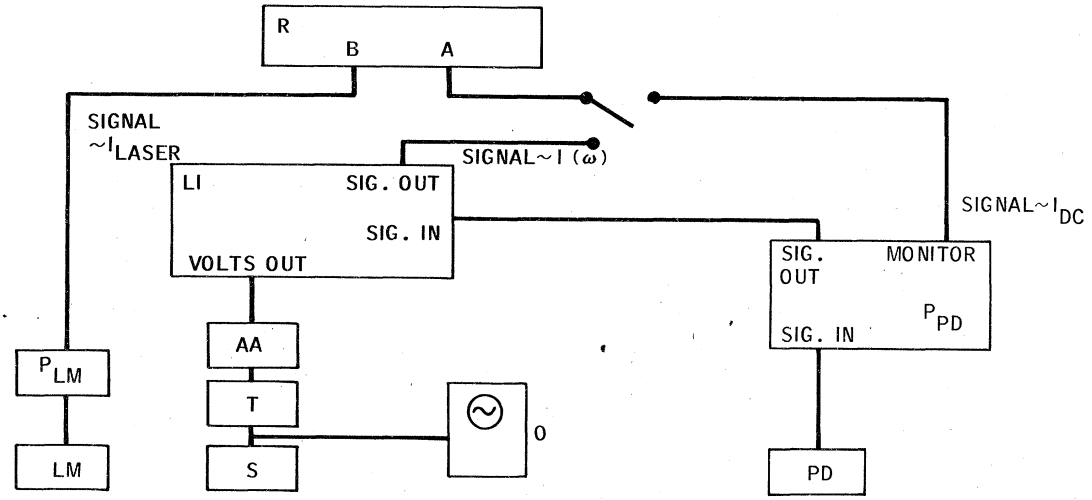

FIG. 3. Block diagram of electronics: AA, audio amplifier; LI, lock-in amplifier; LM, laser monitor; O, oscilloscope; P_{LM}, P_{PD}, preamplifiers; PD, photodiode; R, ratiometer; S, sample; T, transformer.

oven gives stability of 1 mK for over 10 min—long enough to take data at any temperature. Relative temperature measurements are accomplished with a precision thermistor imbedded in the oven just below the sample chamber and are accurate to better than 1 mK. The oven is mounted on a rotating table so that the angle of incidence of the laser beam on the sample can be varied.

A block diagram of the signal measuring electronics is shown in Fig. 3. The lock-in amplifier provides both the field to be applied to the sample and the phase-sensitive detection of the electro-optical signal from the photodiode. Using the lock-in amplifier as a highly accurate (±0.1°) phase measurement device poses several problems. Internal phase shifts within the lock-in are frequency dependent and important even at frequencies as low as 5 kHz. These internal phase shifts vary, for instance, with the setting of the sensitivity of the signal channel. Although the lock-in used can synchronize the reference channel on an incoming sinusoidal signal, this feature introduces phase error because the voltage comparator circuit used causes the reference signal sent to the mixer to have a phase lag (relative to the actual sync input) which is dependent on the amplitude of the sync signal. Further, the Q of the band-pass filter on the signal channel must be turned down to 10 so that small drifts in the center frequency of the filter do not cause phase errors. Due to these problems, the measurement of the phase of the electro-optical response is always made on the same sensitivity setting; and the lock-in itself is used to generate the fields to be applied to the sample.

To measure the ac component of the electro-optical signal, $I(\omega)$, a dc voltage proportional to $I(\omega)$ (at the output of the lock-in amplifier) is divided by the laser monitor signal. When the dc intensity I_{dc} incident on the photodiode is to be measured, these measurements are also divided by the laser monitor signal.

For a given voltage, the field inside the sample cell is difficult to determine accurately. The ac signal to be applied to the sample is produced by the lock-in. An audio amplifier and a transformer are used to step up the voltage to the levels needed. Since the wire separation in the sample is 12 times the wire diameter, the field should be fairly uniform in the center of the cell where the laser beam monitors the modulation of the birefringence. While the field at the center of the cell is uniform, unknown and complicated screening and conduction processes—all frequency dependent—may affect the magnitude of the field. For approximate analysis, these frequency dependences will be neglected.

The amplitude and phase of the electro-optical signal are recorded from 0.5 K below the transition to about 15 K above the transition. The time of each measurement is recorded. To check the linearity between the induced tilt and applied field, the signal is remeasured with the applied voltage reduced by a factor of 2. Nonlinearities are not seen in any of the runs. After each hour of a run, the sample is cooled to a point just above the transition. Data is taken at that temperature and at the five to seven succeeding temperatures. This allows measurement of any drift in the transition temperature. The sample is then warmed back up and the temperature scan proceeds from where it was interrupted.

VI. EXPERIMENTAL RESULTS AND DATA ANALYSIS

Since DOBAMBC is susceptible to minor degradation, the chiral smectic-*A*–smectic-*C* transition temperature decreases during the experiment. Despite this drift of the transition, no visible degradation of sample alignment or condition occurs.

The drift of the transition is measured by periodically monitoring the near transition behavior of the electro-optical response. Figure 4(a) shows the raw data for the phase measurements of a particular run near the transition. As the transition temperature decreases during the run, the data appears to be simply translated parallel to the temperature axis. For such a narrow range of phase, the data closely fit straight lines. Each subset of data is fit to a straight line. From the slopes and intercepts of the fitted lines and with the assumption of a linear drift of T' with time, a single drift rate for T' is found. As shown in Fig. 4(b), a single drift rate brings all the phase data into excellent agreement. For the various experimental runs, the drift rate varies from 6 to 12 mK/h.

Since the chiral smectic-*A*–smectic-*C* phase change is second order, most easily accessible quantities do not exhibit highly distinctive behavior at the transition. Fortunately, the electro-optical response provides a good measure of T'. As shown in Fig. 5, both the phase and amplitude show obvious discontinuities at T'. At lower frequencies, the discontinuity is larger. The width of the discontinuous region is about 20 mK. The reasons for the finite width of this region are not clear. However, the width may be an indication that the correlation length of the fluctuations has become comparable to the helical pitch within the fluctuations (i.e., the temperature regime ΔT has been entered) and the simple spacially homogeneous theory no longer holds.

Figures 6 and 7 show typical data. All data sets show the proper qualitative behavior as described earlier. While data for various frequencies are plotted on the same amplitude graph,

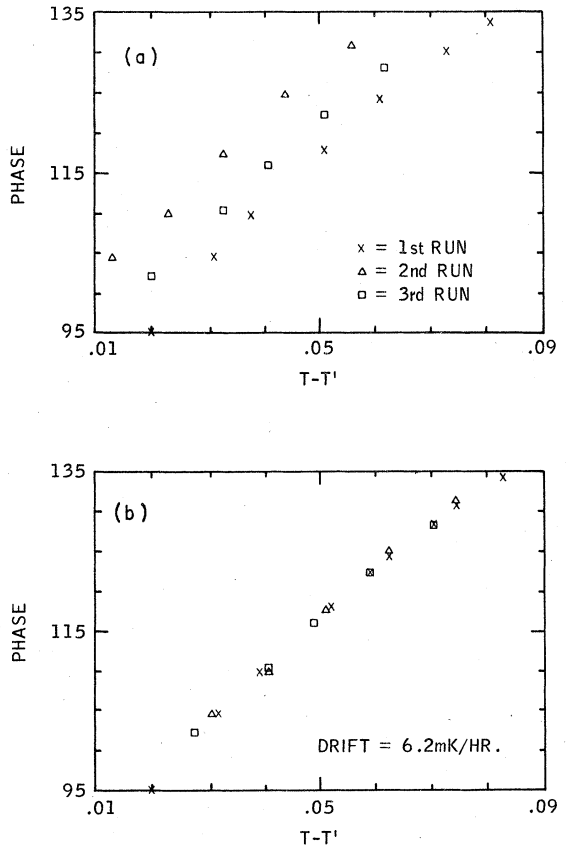

FIG. 4. (a) Phase of the EC effect near T'—uncorrected for drift of T'. Frequency of applied field is 7 kHZ. (b) Phase of the EC effect near T'—corrected for drift of T'.

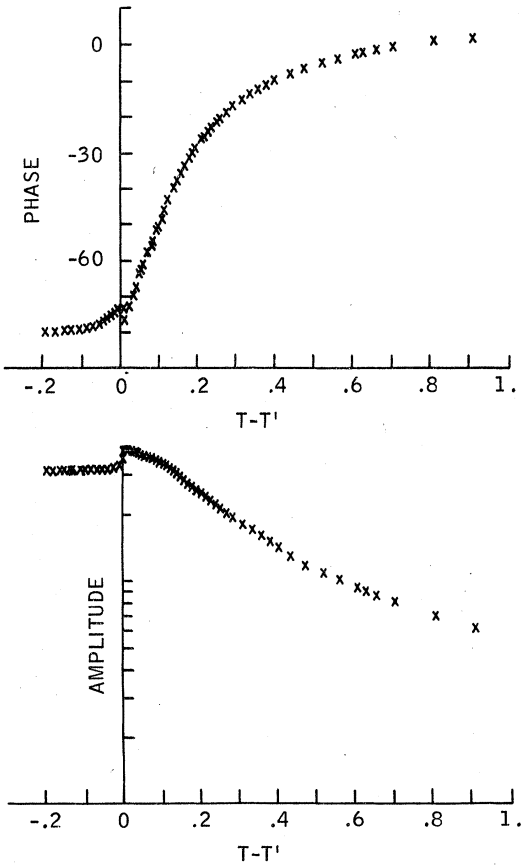

FIG. 5. Discontinuity in EC effect at T'. Frequency of applied field is 20 kHZ.

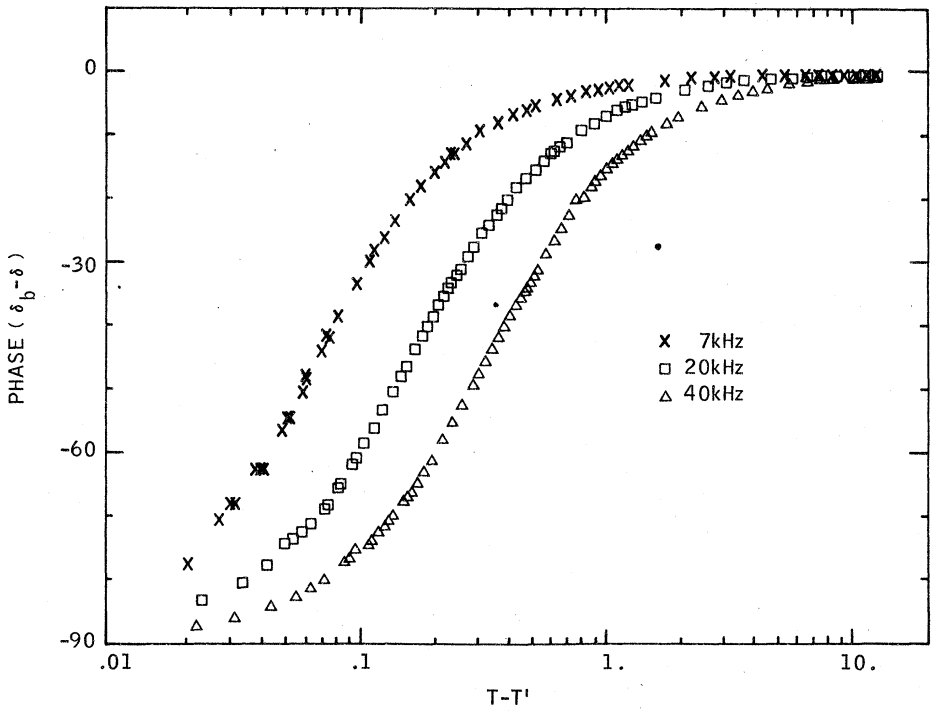

FIG. 6. Typical phase data for three frequencies of the applied field.

comparison of relative magnitudes of the curves may be slightly in error due to the unknown frequency-dependent screening effects in the sample modifying the magnitude of the applied field.

The parameters in Eqs. (9) and (10) are determined from the data by a least-squares analysis. Equation (10) for the phase may be rewritten

$$\ln\tan(\delta_b - \delta) = B/T - \ln(\omega\Gamma/a) - \gamma\ln[(T - T')/T'], \tag{12}$$

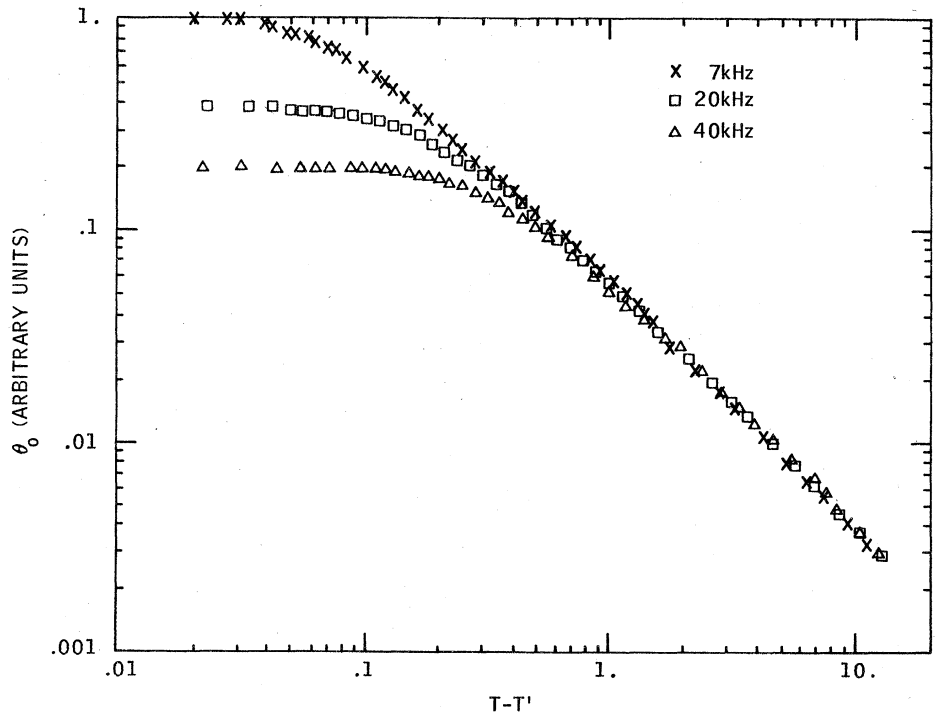

FIG. 7. Typical amplitude data for three frequencies of the applied field.

where δ_b is the constant background phase of the electronics. For each set of B, T', and δ_b, the amplitude and phase data are fitted by nonlinear and linear techniques, respectively.[24] Due to the shape of the χ^2 (reduced mean-square deviation) hypersurface, T', δ_b, and B cannot be reliably fit by the least-squares algorithms used; therefore these three dimensions of the hypersurface are searched externally to the main interations of the least-squares search. The parameter T' found by this technique is the temperature toward which the EC response diverges. It is close to, but not the same as, the phase transition temperature T_c. If the discontinuities in the EC response near T_c are indeed an indication of the temperature regime ΔT, then the fitted parameter T' is about 20 mK from T_c.

Weighting functions for the data are derived from the fact that each phase measurement has the same *absolute* error and each amplitude measurement has the same *relative* error. To explore the theoretical possibilities for γ (discussed earlier), complete fitting procedures were done for (a) $\gamma = 1.315$; (b) $\gamma = 1.0$; (c) γ is an unknown constant; and (d) γ is the crossover function between 1.0 and 1.315 with only the position of the curve along the $\log_{10}[(T - T_c)/T_c]$ axis being adjustable.[21]

Only a limited range of values for the parameters δ_b, B, and T' make physical sense. T' must lie within the discontinuous region of the phase and amplitude data. Far from T', the phase of the electro-optical signal clearly reaches some maximum value. The background phase shift of the electronics δ_b must be at or slightly above this value. Examining 24 nematic compounds, Flanders found that the activation energy for the twist viscosity was between 3700 and 7800 °K.[25] In the fitting procedure used here, B was allowed to vary between 2000 and 9000 °K. This wide range of values for the activation energy certainly covers any value that the viscosity in the dynamic equation (7) may acquire in DOBAMBC.

When fitting with a temperature-independent exponent γ, care must be taken because some of the experimental points may lie in the region having mean-field behavior while other points may lie in the critical region. To this end, fitting is done for subsets of the full data set formed by truncating the data at the near and/or far from T' extremes. This truncation procedure has no effect on the parameters derived from the fitting in this experiment. However, in no case is data nearer than 20 mK to T' used due to the unclear meaning of the "glitches" in the phase and amplitude curves near T'.

In such a multiparameter fit, when the form of the fitting function as well as the values of the parameters are under scrutiny, the criteria for "best" fit are difficult to choose. Finding the minimum χ^2 is not always the optimum technique. In several of the data sets, the minimum χ^2 occurs outside the physically allowed ranges of T', δ_b, and B defined earlier. Increases in χ^2 as large as 30% are needed to bring these variables back to physically reasonable values. Luckily, these changes in the parameter set away from the parameter set which actually minimizes χ^2 cause only very small changes in the final parameters—at most 8% in the critical exponent γ and 12% in the relaxation time τ. Thus the absolute minimum in the full χ^2 hypersurface is not used; however, for the triplet of values δ_b, T', B chosen, the absolute minimum in χ^2 with respect to the other parameters is used.

Figures 8 and 9 show a typical data set and the fitted curves. The error bars on the data needed to account for all statistical fluctuations in the data indicate very small errors: 0.3° error in the phase measurement and 1.5% in the amplitude measurement.

Despite all efforts in varying parameters and truncating data sets, the least-squares analysis with γ as a temperature-independent, adjustable parameter fits the data better than either $\gamma = 1.0$, or $\gamma = 1.315$, or γ for crossover. Although this conclusion is evident when observing the quality of the fits on graphs of the phase or amplitude, it is most easily confirmed by plots of $\ln[(T - T')/T']$ vs $\ln\tan(\delta_b - \delta)$ such as Fig. 8. On such plots, the slope of the data deviates strongly from the slope of the fitted curve with $\gamma = 1.0$ or $\gamma = 1.315$. Further, when using γ for crossover, the slope

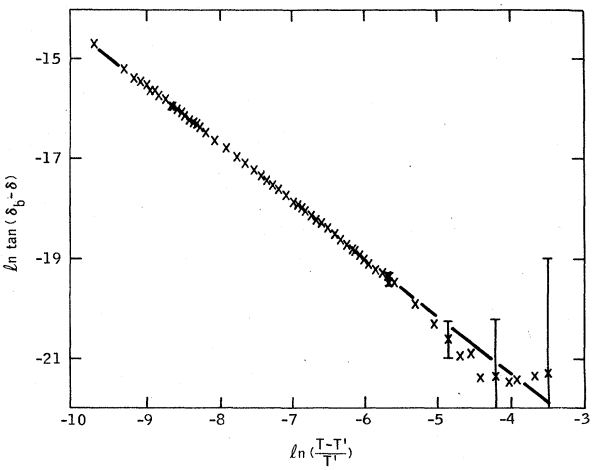

FIG. 8. Fitted curve for the phase data: ln tan $(\delta_b - \delta)$ vs ln $[(T - T')/T']$. Frequency of the applied field is 10 kHz. For this fitted curve $\gamma = 1.13$. Error bars are printed for every fifth point far from T'. Near T', the error bars are much smaller than the characters indicating the data points.

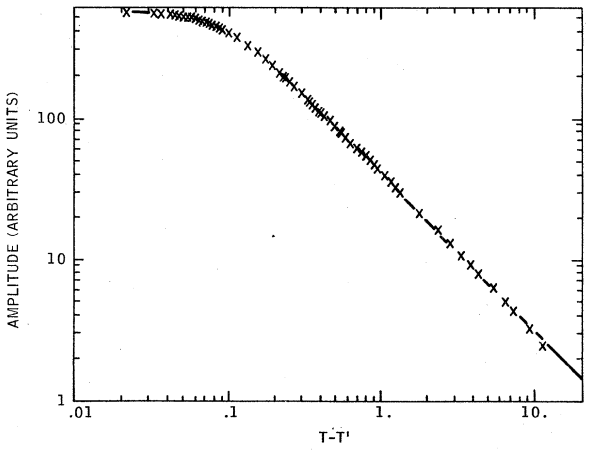

FIG. 9. Fitted curve for the amplitude data. Frequency of the applied field is 10 kHz. For this curve $\gamma = 1.12$. Error bars are much smaller than the characters indicating the data points.

of the fitted curve (which now varies with $T - T_c$ according to a fixed functional form[21]) cannot match the slope of the data over the entire temperature range. Clearly, the fitting in Fig. 8 does not exhibit any of these problems.

The exponent determined from the data analysis is $\gamma = 1.11 \pm 0.06$. The uncertainty for each set of data is slightly smaller than 0.06; however, some small discrepancies do occur for the values obtained from different runs. No dependence on the minor impurity levels in the samples or on the frequency of the applied field is found.

The relaxation time at 0.1 K above T_c is found from the analysis to be 15 ± 2 μsec. Typically, the viscosity of a liquid crystal is on the order of 10 cP.[26] Then from Eq. (11), A is about 10^4 cgs units at 0.1 K above T_c. At absolute zero, the coherence length is

$$\xi(T=0) = (K/a)^{1/2}, \tag{13}$$

where K is an elastic constant (typically 10^{-6} dyn).[27] From the experimental results $\xi(T=0)$ is 4 Å—this is about one molecular dimension, as it should be. For an applied field at 5 kHz, the amplitude of the EC effect is on the order of 10^{-3} rad cm/V very near the transition ($T - T' \sim 30$ mK).

VII. DISCUSSION

The experimental data clearly shows a divergent behavior for the electroclinic response as the chiral smectic-A–smectic-C phase change is approached from the high-temperature side. The behavior can be described by a single exponent γ over the temperature range from 20 mK above the transition to about 15 K above the transition. Within 20 mK of the transition, the electroclinic response deviates from the simple behavior predicted by the spacially homogeneous free energy of Eq. (1). This 20-mK temperature regime is associated with ΔT—the temperature range where the correlation length of the fluctuations is comparable to or greater than the helical pitch within the fluctuations. The exponent γ governing the truncated divergence of the EC coefficient is calculated. In the analysis, data very near T_c are omitted. The divergent behavior of the EC coefficient outside of this temperature regime is interpreted as a measure of the divergence of the true generalized susceptibility of the chiral smectic system. Comparison of the measured value of this exponent

$$\gamma = 1.11 \pm 0.06$$

with the theoretical calculations for the normal-to-superfluid transition in the ^{4}He is not a definitive statement on the analogy between the ^{4}He and chiral smectic transitions. Rather, the discrepancy indicates that (i) although the EC response may be adequately described by a spacially homogeneous free energy except very near T_c, the helical nature of the low-temperature phase influences—in some manner—the EC response and the general critical behavior of the system; and (ii) the critical behavior at this transition cannot be adequately described by a mean-field theory. To further clarify this situation, measurements closer to T_c must be made and the pretransitional behavior of the helical structure of the fluctuations in the chiral smectic-A phase must be investigated.

Beyond the exploration of critical phenomena near the smectic-A–smectic-C transition, this experiment investigates the nature of a new phenomenon in liquid crystals—the electroclinic effect. The linear electro-optical effect originating in the electroclinic effect is a new process to be added to the family of electro-optical responses in liquid crystals. Just as the existence of piezoelectricity is a necessary (although not sufficient) condition for the existence of ferroelectricity in a crystal, the electroclinic effect would have to be present in the ferroelectric smectic-C phase. Further, the pretransitional divergence of the electroclinic response of the smectic-A phase gives clear indication of the Curie point characteristics of the chiral smectic-A–smectic-C transition. Thus the existence and behavior of the electroclinic effect adds consistently to the growing picture of the ferroelectric liquid crystalline phases.

ACKNOWLEDGMENTS

We are grateful to P. Keller, L. Liebert, and L. Strzelecki for the preparation and purification

of our sample. We wish to thank Dr. R. Pindak for his helpful discussions, Professor T. Lubensky, Dr. D. Nelson, and Professor B. Halperin for their comments on the theory of the phase change, and Professor D. Jasnow for the necessary data to generate the crossover function used in our analysis. This research was supported by the Joint Services Electronics Program, by the National Science Foundation through Grant Nos. NSF-SMR76-22452 and NSF-DMR76-01111, and by the Division of Applied Science, Harvard University.

---

*Present address: Exxon Research and Engineering Co., P. O. Box 45, Linden, N. J. 07036.

[1]R. B. Meyer, L. Liebert, L. Strzelecki, and P. Keller, J. Phys. Lett. (Paris) 30, 69 (1975).

[2]P. Keller, L. Liebert, and L. Strzelecki, J. Phys. (Paris) 37-C3, 27 (1976).

[3]Ph. Martinot-Lagarde, J. Phys. (Paris) 37-C3, 129 (1976).

[4]Ph. Martinot-Lagarde, J. Phys. Lett. (Paris) 38, L17 (1977).

[5]B. I. Ostrovskii *et al.*, JETP Lett. 25, 70 (1977).

[6]P. Pieranski, E. Guyon, and P. Keller, J. Phys. (Paris) 36, 1005 (1975).

[7]L. Petit, P. Pieranski, E. Guyon, C. R. Acad. Sci. Paris, Sec. B 284, 535 (1977).

[8]L. J. Yu *et al.*, Phys. Rev. Lett. 36, 388 (1976).

[9]C. Y. Young *et al.*, Phys. Rev. Lett. 40, 773 (1978).

[10]C. Rosenblatt *et al.*, Phys. Rev. Lett. (to be published).

[11]A. Michelson, L. Benguigui, and D. Cabib, Phys. Rev. A 16, 394 (1977).

[12]A. Michelson, Phys. Lett. 39, 464 (1977).

[13]S. Trimper, Phys. Status Solidi B 82, K75 (1977).

[14]S. Garoff and R. B. Meyer, Phys. Rev. Lett. 38, 848 (1977).

[15]S. Garoff, PhD. thesis, *Ferroelectric Liquid Crystals* (Harvard University, Cambridge, Mass., 1977), pp. 1–13 to 1–16.

[16]R. B. Meyer, in *Molecular Fluids Les-Houches 1973*, edited by R. Balian and G. Weill (Gordon and Breach, New York, 1976), pp. 316–320.

[17]V. Dvorâk, Ferroelectrics 7, 1 (1974).

[18]T. Ikeda, Phys. Status Solidi A 16, 279 (1973).

[19]P. G. de Gennes, *The Physics of Liquid Crystals* (Clarendon, Oxford, 1974), pp. 315–316.

[20]P. Pfeuty *et al.*, Phys. Rev. B 10, 2088 (1974).

[21]The crossover from critical to mean-field limits is shown by the dashed curve in Fig. 5 of S. Singh and D. Jasnow, Phys. Rev. B 11, 3445 (1975). This curve is calculated using a Padé approximate to the high-temperature susceptibility of the *XY* model of an fcc lattice with $K_c = 0.2996$ and $\gamma = 1.315$.

[22]F. Brochard-Wyart, PhD. thesis, *Properties Dynamiques des Mesomorphes* (Universite de Paris–Sud, Centre de Orsay, 1974), p. 127.

[23]M. Delaye and P. Keller, Phys. Rev. Lett. 37, 1065 (1976).

[24]P. R. Bevington, *Data Reduction and Error Analysis for the Physical Sciences* (McGraw-Hill, New York, 1969), pp. 232–246.

[25]P. J. Flanders, Mol. Cryst. Liq. Cryst. 29, 19 (1974).

[26]See Ref. 19, pp. 164, 183.

[27]See Ref. 19, p. 64.